Int. J. Multiphase Flow Vol. 18, No. 3, pp. 337–352, 1992
Printed in Great Britain. All rights reserved

0301-9322/92 $5.00 + 0.00

PARTICLE INTERACTION IN THREE-PHASE POLYDISPERSE FLOWS

V. V. DUBROVSKY, A. M. PODVYSOTSKY and A. A. SHRAIBER
Institute of Energy Saving Problems of the Ukrainian Academy of Sciences, Kiev, Ukraine

(Received 20 September 1990; in revised form 12 December 1991)

Abstract—A systematic experimental study of the interaction of drops with solid particles of different sizes moving with moderate and high relative velocities has been carried out. It has been stated that collisions are commonly accompanied by liquid breaking up and forming a certain amount of polydisperse fragments. The generalizing formulae are obtained for the parameters of the material balance of interaction and also for the fragments' sizes and velocities. Based on the experimental results, numerical studies of three-phase polydisperse flow characteristic properties have been carried out.

Key Words: drops, solid particles, interaction, collision, coalescence and breakup, three-phase flow, aggregate, mass transfer

1. INTRODUCTION

Flows of three-phase mixtures consisting of gas and liquid drops and solid particles suspended in it, are widely spread in nature and engineering, e.g. the motion of water drops and ice particles in the atmosphere, the simultaneous burning of liquid and solid fuels, processes of liquid application on the surface of solid particles, three-phase working medium expansion in rocket and jet engines etc. The discrete phase state evolution is determined by the interaction of drops and their destruction by aerodynamic forces in two-phase (gas–liquid drops) flows (Podvysotsky & Shraiber 1984; Nigmatulin 1987; Pilch & Erdman 1987). At the same time, three-phase polydisperse flow presents a considerably richer and more varied physical pattern. Two-component particles (aggregates) consisting of liquid and solid inclusions are always formed in three-phase flow. Because of this, the interaction of pure drops and solid particles, the collision of aggregates with each other and with pure particles and the destruction of aggregates by aerodynamic forces etc. should be referred to as the "elementary" physical phenomena.

It has been shown in the review by Shraiber (1988), that when modelling the three-phase medium state evolution it is most advisable to use the continuous approach to describe particle interaction (Gillespie 1975) and the Lagrangian method (Sternin *et al.* 1980). This allows us to avoid separate consideration of pure and two-component particles and to confine ourselves to the analysis of the change of state of two polydisperse ensembles: (a) the aggregates with liquid basis (particles of the first type)—these particles had been pure liquid ones in the inlet section, then they combined with a certain amount of smaller particles of different structures; (b) the aggregates with solid basis (particles of the second type)—particles which had been solid ones in the inlet section (henceforth these aggregates will be termed drops and solid particles, respectively). As the continuous approach provides different descriptions of the mass transfer upon collisions of i particles with smaller or larger ones (Sternin *et al.* 1980; Vasenin *et al.* 1986), the adopted scheme of the flow disperse mass component composition results in the need to consider the following four kinds of interaction:

(1) interaction of two drops, $\delta_j - \delta_i$ ($\delta_j < \delta_i$);
(2) interaction of a small drop with a large solid particle, $\delta_j - \Delta_i$ ($\delta_j < \Delta_i$);
(3) interaction of a small solid particle with a large drop, $\Delta_j - \delta_i$ ($\Delta_j < \delta_i$);
(4) interaction of two solid particles, $\Delta_j - \Delta_i$ ($\Delta_j < \Delta_i$).

Here δ, Δ represent the particle diameter—values that refer to the drops are defined by lower-case letters and those which refer to solid particles are defined by capital letters. The smaller of two interacting particles we shall call a projectile, the larger one—a target. Let us introduce the coalescence and breakup parameter for each kind of interaction (Φ_{ji}, X_{ji}, Ψ_{ji}, Ω_{ji}, respectively), this parameter being the mathematical expectation of the ratio between the target mass change during some time τ and the total mass of projectiles colliding with it (Podvysotsky & Shraiber 1984), and the coalescence constant (K_{ji}, L_{ji}, P_{ji}, N_{ji}). For instance, for the X-interaction we have

$$L_{ji} = E^{X}_{ji}(\Delta_{ji} + \delta_j)^2 \frac{|u_j - U_i| g_j}{u_{ij}}, \qquad [1]$$

where E is the collision efficiency, u, U represent the velocity and g is the drops' distribution function by masses m [$\mathrm{d}w_j = g(m_j)\,\mathrm{d}m_j$, $g_j = g(m_j)$; w is the mass rate concentration].

The full set of equations of the flow discrete mass state evolution includes the equations relative to masses m, M, distribution functions g, G, velocities u, U, temperatures t, T and liquid contents b, B for drops and solid particles. Let us cite as an example the one-dimensional, stationary equations for m and g (Shraiber & Dubrovsky 1986; Shraiber 1988; Shraiber & Klimov 1989):

$$\frac{\mathrm{d}m_i}{\mathrm{d}x} = \frac{\pi u_G \rho_G}{4u_i} \int_0^{m_i} (K_{ji}\Phi_{ji}\,\mathrm{d}m_j + P_{ji}\Psi_{ji}\,\mathrm{d}M_j); \qquad [2]$$

and

$$\frac{\partial g_i}{\partial x} + g_i \frac{\partial}{\partial m_i}\left(\frac{\partial m_i}{\partial x}\right) = \frac{g_i}{m_i}\frac{\mathrm{d}m_i}{\mathrm{d}x} + \frac{\pi u_G \rho_G}{4} \int_{m_i}^{\infty} \left\{ \frac{g_k}{m_k u_k}\left[\int_0^{m_k} (K^0_{jki}\,\mathrm{d}m_j + P^0_{jki}\,\mathrm{d}M_j) - K_{ik}\right]\mathrm{d}m_k \right.$$

$$\left. + \frac{G_k}{M_k U_k}\left[\int_0^{M_k} (L^0_{jki}\,\mathrm{d}m_j + N^0_{jki}\,\mathrm{d}M_j) - L_{ik}\right]\mathrm{d}M_k \right\}. \qquad [3]$$

Here ρ is the density, $\psi^0_{jki} = \psi_{jk}(1 - \omega_{jk})\alpha^{\omega}_{jki}$ (for the four kinds of interaction, respectively: $\psi = K$, L, P, N; $\omega = \Phi$, X, Ψ, Ω); α^{ω}_{jki} is the mass function of liquid i fragments distribution at the ω-interaction of j and k particles, the index G refers to carrying gas. On the right-hand side of [3], the first term allows for the interaction of i drops with smaller particles, the other terms allow for the formation of i fragments under various interactions and the disappearance of i particles due to their collisions with larger particles. To use the described model in practice, it is necessary to obtain information on the mass and impulse transfer in interactions of particles of the same and different natures (the functions Φ, X, α etc.). The next section will present a brief analysis of the results available in this field. Since we consider the case of rather high relative velocities, let us suppose that physical contact between the particles is always achieved by a collision. To simplify further, we consider these particles as electrically neutral ones. Hence the influence of such factors as thermo- and diffusiophoresis, flow fields around the particles, their charge etc. are not considered here. These problems are presented in detail in the literature (Pruppacher & Klett 1978; Martin *et al.* 1980; Czys & Ochs 1988 etc.).

2. RELATED LITERATURE

As far as we know, the interaction of two-component particles has not been studied at all, and collisions of pure particles with aggregates have not been studied sufficiently. As to the collisions of pure particles between themselves, the Φ-interaction is the one that has received the greatest attention (Pruppacher & Klett 1978; Podvysotsky & Shraiber 1984; Vasenin *et al.* 1986; Ochs *et al.* 1986). For the interaction of drops in a quiescent gaseous medium it is advisable to use the following formula:

$$\Phi_{ji} = 1 - 0.246\,\mathrm{Re}_{ji}^{0.407}\,Lp_i^{-0.096}\left(\frac{\delta_i}{\delta_j}\right)^{-0.278}; \qquad [4]$$

in the range of $30 < \mathrm{Re}_{ji} < 6000$, $5 < Lp_i < 3 \cdot 10^5$, $1.9 < \delta_i/\delta_j < 12$. Here $\mathrm{Re}_{ji} = |u_j - u_i| \delta_j \rho_L / \eta_L$ is the Reynolds number, $Lp_i = \delta_i \rho_L \sigma / \eta_L^2$ is the Laplace number, σ is the coefficient of surface tension, η is the dynamic viscosity and the index L refers to the liquid. Under the action of gas flow, the value of the coalescence and breakup parameter decreases:

$$\Phi_{ji}^0 = \Phi_{ji} - \varphi_{ji}; \quad \varphi_{ji} = \begin{cases} 0.00446 A_{ji}, & A_{ji} < 40.6; \\ 11.85\left(\dfrac{A_{ji}}{100}\right)^{4.64}, & 40.6 < A_{ji} < 120; \end{cases} \qquad [5]$$

where $A_{ji} = \mathrm{Re}_{ji}^{0.285} Lp_i^{0.2} \mathrm{We}_i^{0.442} (\delta_i/\delta_j)^{0.4}$ and $\mathrm{We}_i = (u_G - u_i)^2 \rho_G \delta_i / \sigma$ is the Weber number.

Regularities of the X-interaction have only been studied in sufficient detail with regard to applications to the problems of aerophysics—the collisions of water drops with the surface of hailstones (Pruppacher & Klett 1978; Khorguany 1984; Lew *et al.* 1986; Smirnov 1987). It has been stated that at central impacts not very small drops ($\delta_j \gtrsim 50\,\mu$m) are usually splashed and reflected, and at tangential impacts—the drops slip through the surface and break away from it. With the particle surface being covered with a water film (of thickness d), the liquid splashing becomes more intensive, especially when $\delta_j > d$. It should be noted that under the interaction of water drops with ice particles, such factors as heat transfer between particles, crystallization etc. have a certain effect on the coalescence process. As far as we know, the phenomenon "in pure form" has been studied in only two papers. Gawronski & Roszak (1979) analysed the conditions of drop breakup at a central impact against a spherical surface. The authors assumed that liquid splashing can occur only if the impact kinetic energy is sufficient to form a new surface [note that similar considerations in analysing the impact of two drops were used in the well-known paper by Brazier-Smith *et al.* (1972)]. A more thorough experimental study of the X-interaction was carried out by Zavadsky (1982). Solitary glass balls with $\Delta_i = 2$ mm dia and 40–80 m/s initial velocity were fired through the cloud of drops of a nitrocellulose enamel solution in acetone and then caught by special vessel, filled with toluene. The amount of liquid settled on the balls was calculated from the paint concentration washed out of the particles in the toluene. Unfortunately, Zavadsky (1982) gives no details of the size and concentration of the drops and does not try to generalize the experimental results obtained.

The particle coagulation features of the Ψ- and Ω-interactions have not been studied enough. In this connection only a few papers can be mentioned: Stulov *et al.* (1978), where the behaviour of specks of dust upon impact against the surface of drops is considered; Babukha & Shraiber (1972), where collisions of solid particles with fused surfaces are considered; and Sauter & Wang (1989), where coagulation of the smallest aerosol particles with ice crystals is studied.

Studies of the stability of two-component particles also relate to this question. Davis & Brenner (1981) analysed the stability of a viscous drop containing a solid core with Δ_n diameter in a shear flow. It has been stated that regions exist where the core presence decreases the particle deformation [$H = \eta_1/\eta_G \gg 1$, $K = \sigma/(G\eta_G\delta) \sim 1$; where G is the shear rate] and, on the contrary, it destabilizes the latter and makes its destruction easier ($H \sim 1$, $K \gg 1$). Khorguany (1984) presented an empirical formula for the critical mass m_f of the film on the surface of an artificial hailstone under free fall: $m_f = \alpha \Delta_n^2$ [$\alpha = (0.07 \pm 0.007)$ g/cm^2; m_f in grammes, Δ_n in centimetres]. Similar measuremnts have also been carried out by Rasmussen & Heymsfield (1987), as a result $m_f = 0.268 + 0.139\, m_n$ (m_f and m_n in grammes). Both formulae predict similar values of m_f. Petela & Zajdel (1980) calculate the maximum film thickness which can exist on a spherical particle blown by a gaseous flow from the condition of equality between the forces of surface tension and aerodynamic resistance.

Thus, in the literature there is only scanty information on the quantitative and qualitative regularities of particle interactions in three-phase polydisperse flows. These data are insufficient to develop reliable methods of calculation of three-phase flows in conformity with different applied problems. This paper presents the results of systematic experimental studies of the mass and impulse transfer under X- and Ψ-interactions of pure particles, and also some data on collisions of pure particles with two-component ones.

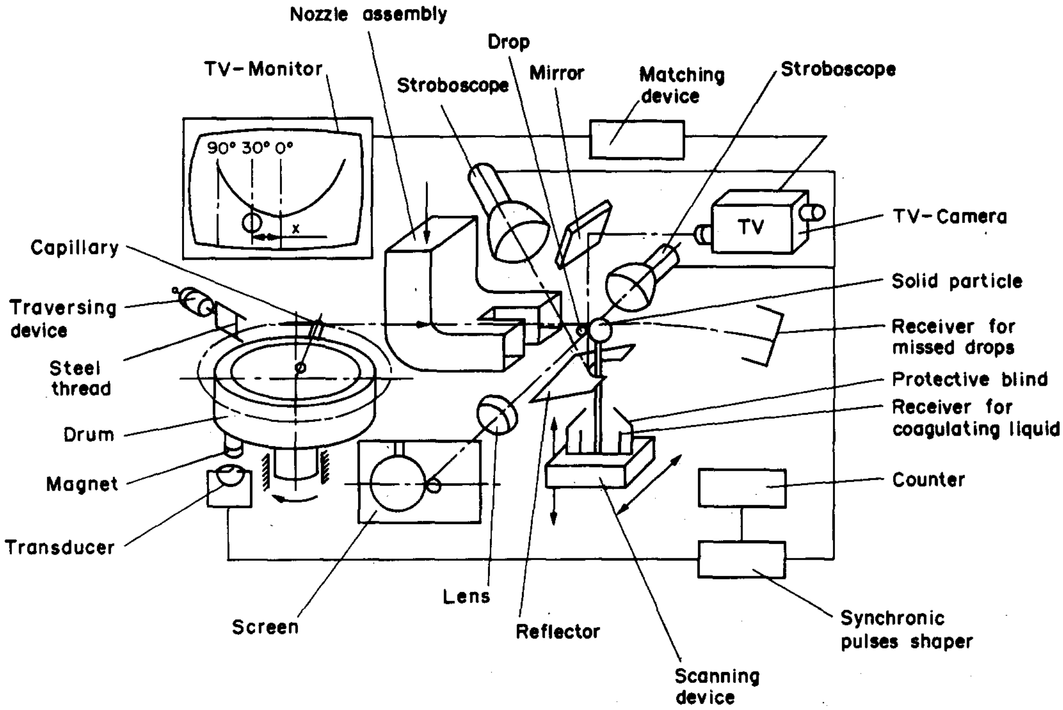

Figure 1. Experimental apparatus for investigation of the interaction between small drops and large solid particles.

3. INTERACTION OF SMALL DROPS WITH LARGE SOLID PARTICLES

3.1. Measurement of averaged values of the coalescence parameter

The experimental apparatus (shown in figure 1) was used to bombard a large spherical solid particle, fixed on fine rack, with small monodisperse drops moving with high velocities. The rotating drum with a capillary was used as the projectile generator. Upon rotation of the drum, the monodisperse drops break away from the capillary end. To stabilize the projectiles' working trajectory in space we used the steel thread attached to the micrometric traversing device. A detailed description of the projectile generator is presented in the paper by Podvysotsky & Shraiber (1984).

The different phases of the drop interaction with the solid particle were visualized in stroboscopic light. External synchronic pulses were used to regulate the stroboscope. These pulses were generated by a shaper at the instant the magnet passed over the transducer. The magnet was attached to the rotating drum. As a result, an absolutely "frozen" picture of the process was obtained in stroboscopic light. The number of drops generated was determined by the counter from the number of drum rotations. To avoid the effect of the fixing rack during the experiment, only the "northern" hemisphere of the solid particle was bombarded.

The coalescence of drops with the surface of the particles depends considerably on the collision angle of the projectile with the target. To obtain directly from the experiment the values of the coalescence parameter X_{ji} corresponding to the equiprobable outcome of the interaction (averaged by the midship section of the target), the solid particle during the bombardment was moved by a scanning device in two mutually perpendicular directions in the plane normal to the trajectory of the projectiles. Because of this each alternate projectile collided with a different point on the target surface. As the period of target bombardment by the drops was sufficiently long, its dry surface was covered gradually with a liquid film, the thickness of which was approximately constant. Thus, the drops collided not with the clean dry surface of the solid particle (with the exception of the initial period of bombardment) but with aggregate (particles of the second type). The scanning amplitude was set somewhat higher than the target radius. The projectiles flying past the solid particle were collected in the receiver for missed drops. Liquid coagulating with the solid particle was separated periodically from the ball surface and slipped through the rack into the

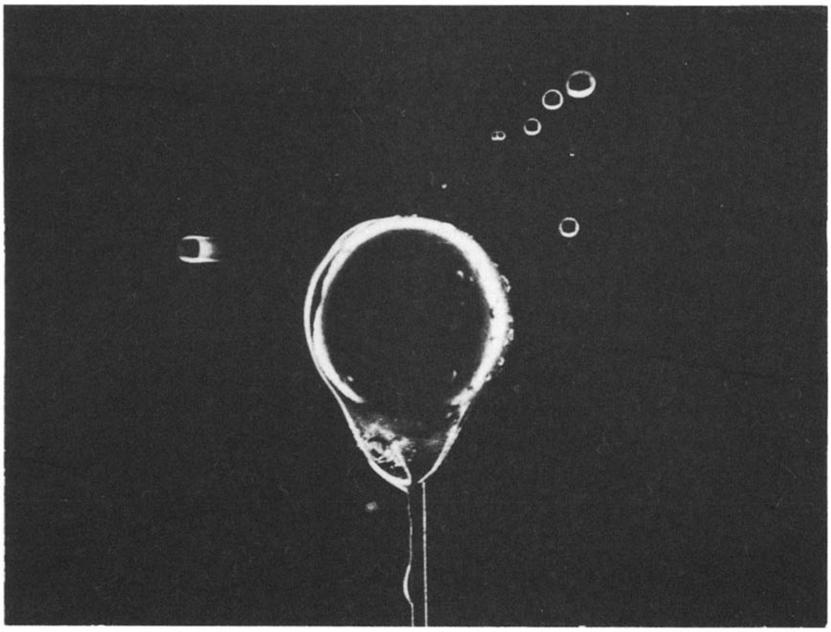

Figure 2. Phases of interaction of the drop with the solid particle at $Re_{ji} = 260$, $Lp_j = 70$, $\theta = 1.38$, $\Delta_i/\delta_j = 7.7$.

receiver for coagulating liquid. The protective blind has prevented fragments from hitting the receiver.

In the experiments, drops with $\delta_j = 0.65$ to 1.05 mm dia and smooth spherical targets with $\Delta_i = 3.2$ to 8.0 mm dia were used. The relative velocity of collisions was in the range $u_j - U_i = 7$ to 10 m/s. Water–glycerine solutions with a glycerine concentration of $C = 0$ to 91% were used as the model liquid, the coefficient of the solutions' dynamic viscosity varying by two orders. The methods of measurement were the same as in the paper by Podvysotsky & Shraiber (1984).

Figure 2 presents two phases of the interaction of the drops with the solid particle (a projectile flying toward the target and the group of fragments formed).

Figure 3 illustrates the dependence of the X_{ji} coalescence parameter on the coefficient of dynamic viscosity. The increase in the viscosity of the drops results in an increase in X_{ji}. The coalescence parameter also increases by increasing the relation between the target and the projectile diameters Δ_i/δ_j.

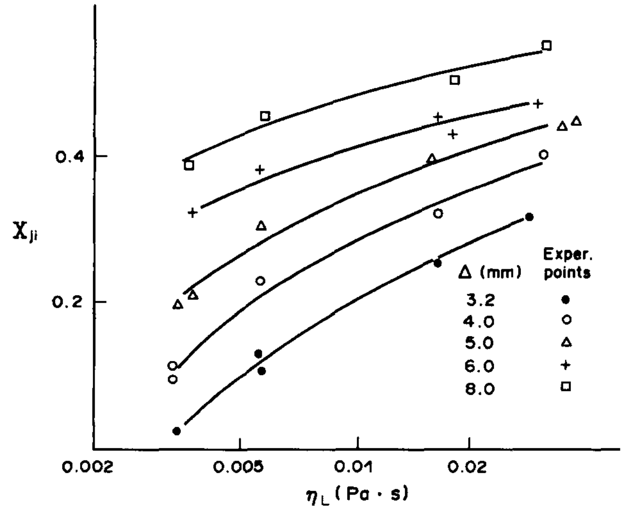

Figure 3. Variation of the coalescence parameter with viscosity at $\delta_j = 0.7$ mm.

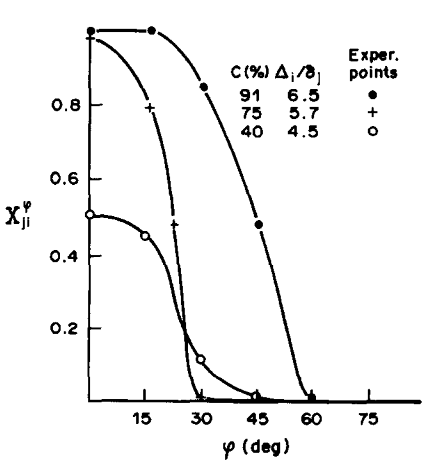

Figure 4. Variation of the X_{ji} parameter local value with the particle collision angle.

It has been found that the parameter X_{ji} is affected by the physical properties of the solid particle surface. With this in mind, the experiments were carried out with targets made from different materials and also with particles covered with hydrophobic films, which changed the wetting conditions on the "solid body–liquid" boundary. The value of the boundary angle θ was found experimentally. The experiments revealed that the effects of the boundary conditions on the interaction outcome are non-significant for wetting surfaces ($\theta < 90°$), especially for high liquid viscosities ($C = 75$ to 91%). For non-wetting target surfaces ($\theta > 90°$), a reasonably sharp decrease in the X_{ji} parameter was observed with increasing θ. In the experiments the maximum boundary angle was 107°. Extrapolating these data to the region of larger values of θ, it can be assumed that $X_{ji} \to 0$ if $\theta \to 180°$.

The treatment of more than 800 experimental points for solid particles made from steel, steel with hydrophobic coatings, acrylic glass, soda-lime glass and fluoroplastic allowed us to obtain the following formula:

$$X_{ji} = \begin{cases} 1 - 0.044B_{ji}, & B_{ji} \leqslant 22.7; \\ 0, & B_{ji} > 22.7; \end{cases}$$

$$B_{ji} \equiv \mathrm{Re}_{ji}^{0.85} Lp_j^{-0.32} \left(\frac{\Delta_i}{\delta_j}\right)^{-0.34} \theta^{0.32}; \qquad [6]$$

in the range $24 \leqslant \mathrm{Re}_{ji} \leqslant 2.5 \cdot 10^3$, $0.7 \leqslant Lp_j \leqslant 3.7 \cdot 10^4$, $3 \leqslant \Delta_i/\delta_j \leqslant 17$, $0.96 \leqslant \theta \leqslant 1.87$ ($55° \leqslant \theta \leqslant 107°$). Here Re_{ji} is determined in the same way as in [4], $Lp_j = \delta_j \rho_L \sigma / \eta_L^2$. The maximum deviation of the experimental points from [6] does not exceed 0.19, the r.m.s. deviation is 0.08. Experiments with compound particles were also carried out, the particles were made by resistance welding of steel balls with a diameter of 1 mm. The difference in the coalescence parameter values for smooth and compound particles did not exceed 0.1 in the range studied, i.e. it is comparable with the experimental error. Thus, [6] can be used to define the coalescence parameter when drops interact with compound particles.

The effect of air flow through the nozzle assembly on the coalescence of the drops with large smooth particles was studied using the apparatus in figure 1. The particle was located at the point of mixing of jets flowing out of the two channels of the nozzle assembly, the air velocity vector being coincident with the direction of the projectile motion. It has been established that aerodynamic forces affect the frequency of the removal of the liquid from the particle and the liquid mass added to it but not the X_{ji} value (Podvysotsky *et al.* 1990).

3.2. Local values of the coalescence parameter

To study the mechanism of the interaction of drops with the solid particles in detail, the measurement of the local values of the coalescence parameter X_{ji}^{φ} is of great interest. These values correspond to fixed angles φ of collision of the projectile with the target (φ is the angle between the line connecting the centres of the interacting particles at the moment of contact and the relative velocity vector). The studies were carried out on the same experimental apparatus (figure 1). However, the scanning device was not used, and during the bombardment the target was fixed. To define the mutual position of the particles at the moment of contact, the plant was equipped with an optical-TV system. Before the experiment the solid particle was set in such a way that the drops' trajectory was situated in the target equator plane. Monitoring was performed by the particle image on the semi-transparent screen obtained with the help of a lens with 10-fold magnification. In the horizontal plane the particle's position was defined by the graticule on the screen of the TV-monitor. In this plane the image reflected from the mirror was transmitted by the TV-camera through the matching device on the monitor. To increase the image contrast range on the monitor screen a dispersive screen-reflector was used, which forms the light background for the particles. The angle of a particle collision was determined by the expression $\varphi = \arcsin[2x(\delta_j + \Delta_i)^{-1} z^{-1}]$, where x is the perpendicular distance between the target centre and the projectile trajectory measured on the monitor screen and z is the increase ratio.

Figure 4 shows a typical view of the experimental curves. In the region studied, after the nearly central collisions ($\varphi \approx 0$) intensive coagulation takes place, especially for the case where the drops

Table 1. Values of the coefficients in [8]

Parameters	Coefficients			
	α	β	γ	ζ
A	14.4	−0.74	0.27	0.39
B	0.94	−0.05	−0.1	0.58
D	$2.2 \cdot 10^{-7}$	4.82	−2.18	0.26
F	97	−2.25	0.54	1.11
$\ln \bar{\varepsilon}$	−0.16	0.63	−0.31	−0.11
$\ln \Sigma$	83.4	−1.34	0.6	0.17

are viscous. In the latter case, a horizontal section of the curve $X_{ji}^{\varphi}(\varphi)$ was detected at small φ angles for sufficiently large targets. The extent of this section increased with growth of the relation Δ_i/δ_j. With increasing φ, the local values of the coalescence parameter reduced to zero.

The experimental data analysis showed that on the coordinates $(1 - X_{ji}^{\varphi})/(1 - X_{ji}) - \varphi$, the experimental points can be sufficiently well-approximated by the relations

$$\frac{1 - X_{ji}^{\varphi}}{1 - X_{ji}} = \begin{cases} A - B\exp[-D(\varphi - F)^3], & \varphi \geqslant F; \\ A - B, & \varphi < F; \end{cases} \qquad [7]$$

$$\Psi = \alpha \mathrm{Re}_{ji}^{\beta} Lp_j^{\gamma} \left(\frac{\Delta_i}{\delta_j}\right)^{\zeta} (\psi = A, B, D, F) \qquad [8]$$

(the values α, β, γ and ζ are tabulated in table 1). Relation [7] is true in the range of $35 \leqslant \mathrm{Re}_{ji} \leqslant 1.5 \cdot 10^3$, $1.5 \leqslant Lp_j \leqslant 5.2 \cdot 10^3$, $3.2 \leqslant \Delta_i/\delta_j \leqslant 11.4$. The maximum deviation of the experimental points did not exceed 0.1.

3.3. Determination of the initial parameters of secondary particles

Photographic studies allowed us to determine the spectrum of sizes of the fragments (secondary drops) and their motion characteristics. As a result of processing about 10 thousand fragments, it has been determined that the size distribution of the fragments subordinates the lognormal law

$$f(\varepsilon) = \frac{1}{\sqrt{2\pi}\varepsilon \ln \Sigma} \exp\left[-\frac{(\ln \varepsilon - \ln \bar{\varepsilon})^2}{2\ln^2 \Sigma}\right]. \qquad [9]$$

Here $\varepsilon = \delta_k/\delta_j$, δ_k is the fragment diameter, $\bar{\varepsilon}$ is the average relative size of the fragments and $\ln^2 \Sigma$ is the standard deviation of the fragment size logarithm. The values of the distribution [9] parameters averaged over all modes studied were determined ($\ln \bar{\varepsilon} = -1.1$, $\ln \Sigma = 0.57$). To provide more accurate computations $\ln \bar{\varepsilon}$ and $\ln \Sigma$ can be determined from [8] (the coefficient values are given in table 1).

For the mean value of the fragments' initial velocity u_k, the approximate formula was obtained independently of the interaction conditions

$$\frac{\bar{u}_k}{u_j} \approx 0.4,$$

i.e. in this case the fragments assume a higher velocity than under drop interaction (Podvysotsky & Shraiber 1984). This fact is probably connected with the differences in the experimental descriptions—the free-moving targets can acquire a certain amount of the projectile energy, that is why the fragments move more slowly.

4. COLLISIONS OF SMALL SOLID PARTICLES WITH LARGE DROPS

4.1. The experimental apparatus: methods of analysis

The study of the interaction of small solid particles with large drops falling freely was carried out using the experimental apparatus shown in figure 5. The spherical particles were "fired" by

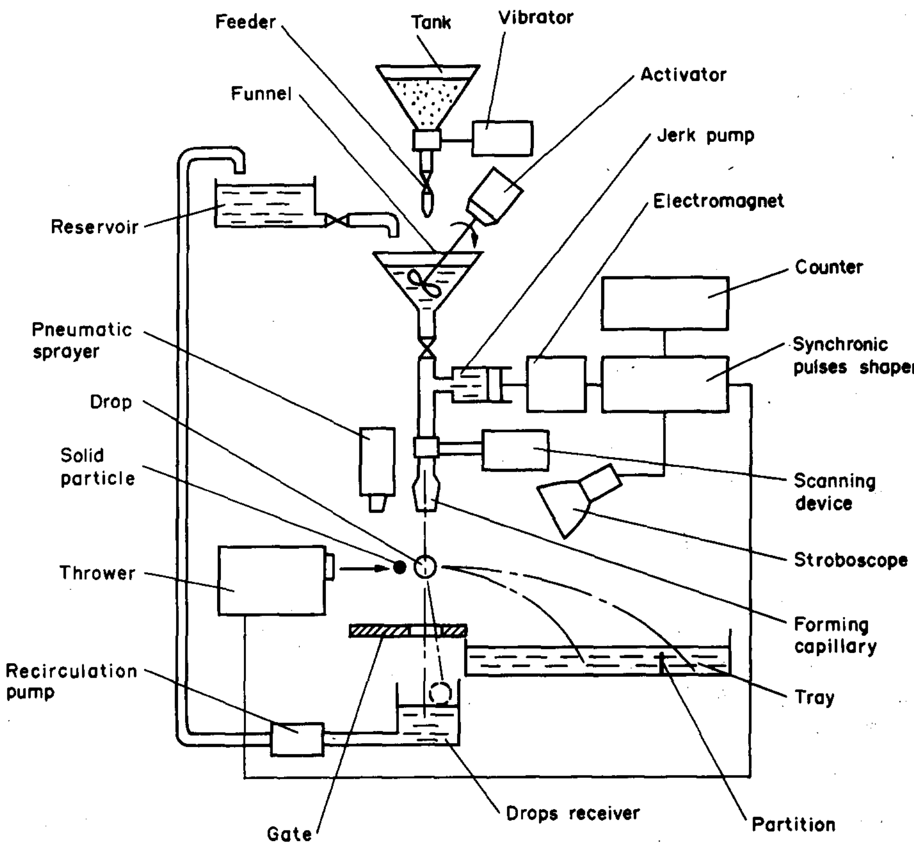

Figure 5. Experimental apparatus for investigation of the interaction between small solid particles and large drops.

a rotor-type thrower under the action of centrifugal forces. The thrower provided a single particle output, flying in a trajectory stable in space, for each rotor revolution. The operating principle of the generator of the drops falling freely (forming capillary, jerk pump, electromagnet), is described in detail in paper by Podvysotsky & Shraiber (1984). In the closed circuit of the target generator (reservoir, funnel, forming capillary, drops receiver, recirculation pump), continuous fluid circulation was maintained, the fluid mass being constant (allowing for a correction for evaporation).

The performance of the solid particles generator and of the drops generator was synchronized to provide a high probability of the particles interaction at the intersection point of the working trajectories. The value of the coalescence and breakup parameter Ψ_{ji}, averaged by the target midship section, was determined. In order to do this, the forming capillary was moved by means of the scanning device (in a similar manner to that described in section 3). During the bombardment, the projectiles which missed the target were collected in a tray behind the separating partition, and those which hit the target were collected in front of the partition. The process was visualized by the stroboscope, which was controlled by the shaper of the synchronous pulses from the solid particles thrower. The number of the particles which escaped from the thrower was determined by the counter. Fragments formed during collisions were prevented from falling into the drops receiver by the gate.

During the experiments, changes in the liquid mass circulating in the target generator circuit were measured, they result from the interaction of particles. The measurments were performed by weighing the whole circuit before and after the experiment (the weight method). The total mass of projectiles colliding with the target was also determined. Water–glycerine solutions with a glycerine concentration of $C = 0$ to 97% were used as the model liquid. The diameter of the drops was $\delta_i = 2.9$ to 5.6 mm, the diameter of the solid particles was $\Delta_j = 1.0$ mm and their density was $\rho_s = 2700$ to 15,200 kg/m^3, the relative velocity was within the range 3.4–12.8 m/s.

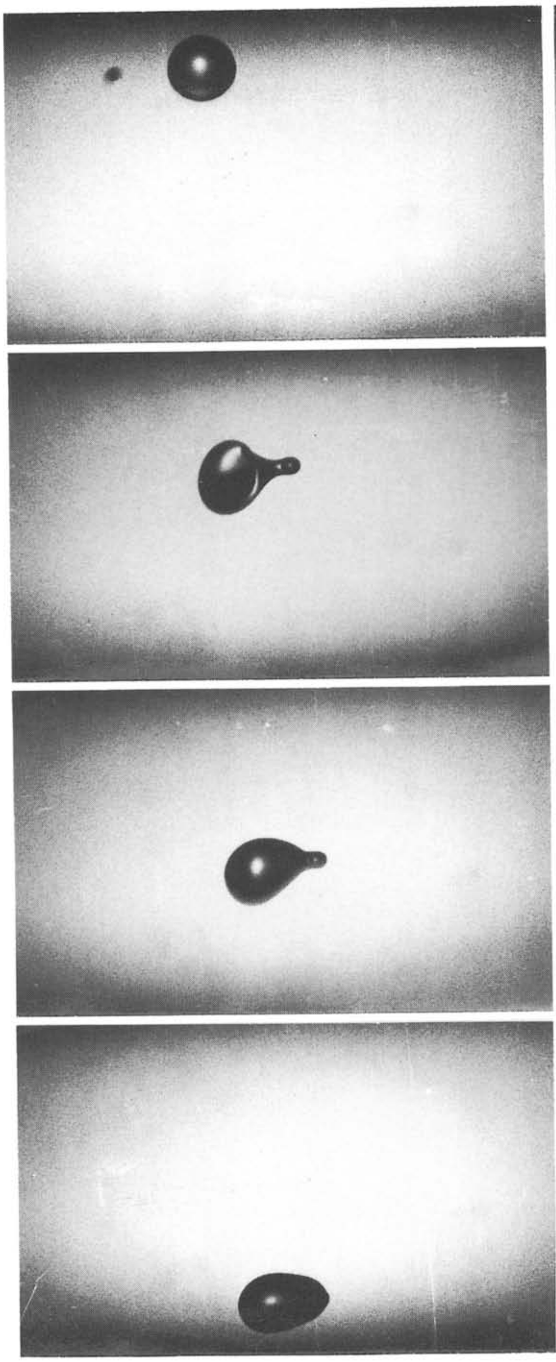

Figure 6. Interaction phases in the capture mode.

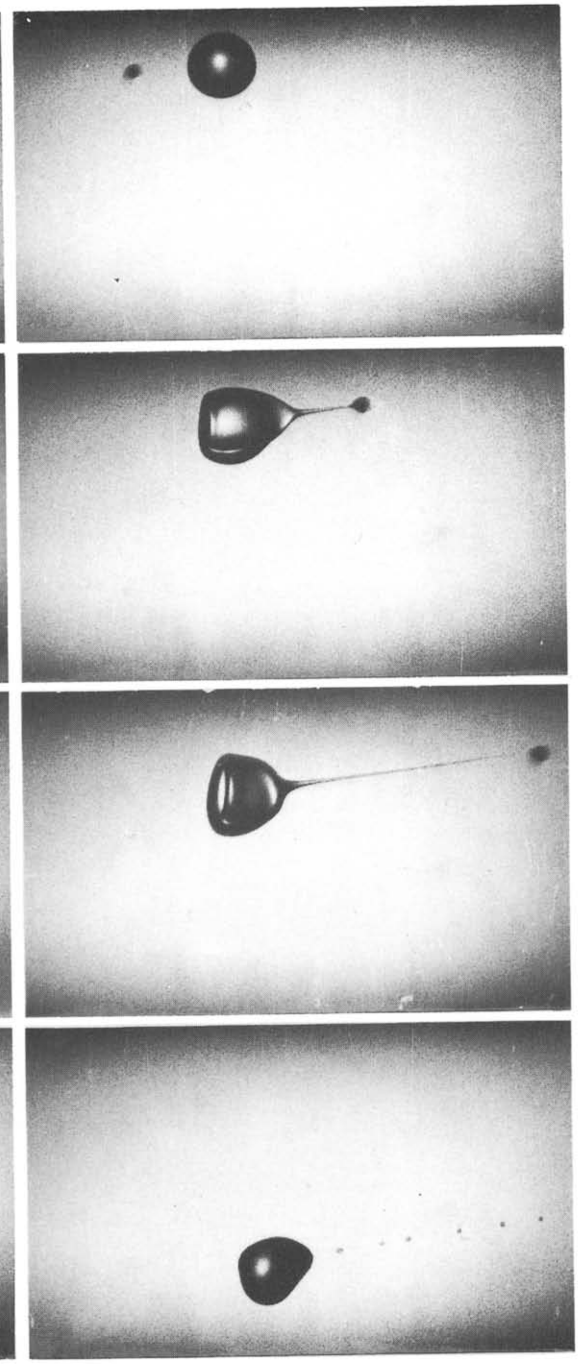

Figure 7. Interaction phases in the "shooting through" mode.

4.2. The interaction modes

As a result of the experiments, four characteristic collision modes have been found:

(1) Solid particle capture by the drop target without fragment formation (complete coagulation, figure 6).
(2) Drops "shooting through" the particle with the formation of an insignificant number of fragments (the target individuality is retained, figure 7).
(3) Formation of an air bubble (hollowness) in the target as a result of interaction (shooting through, figure 8).

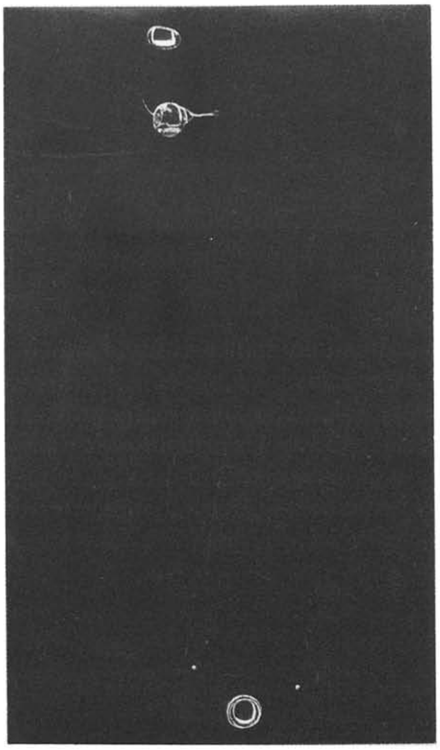

Figure 8. Interaction phases in the bubble formation mode.

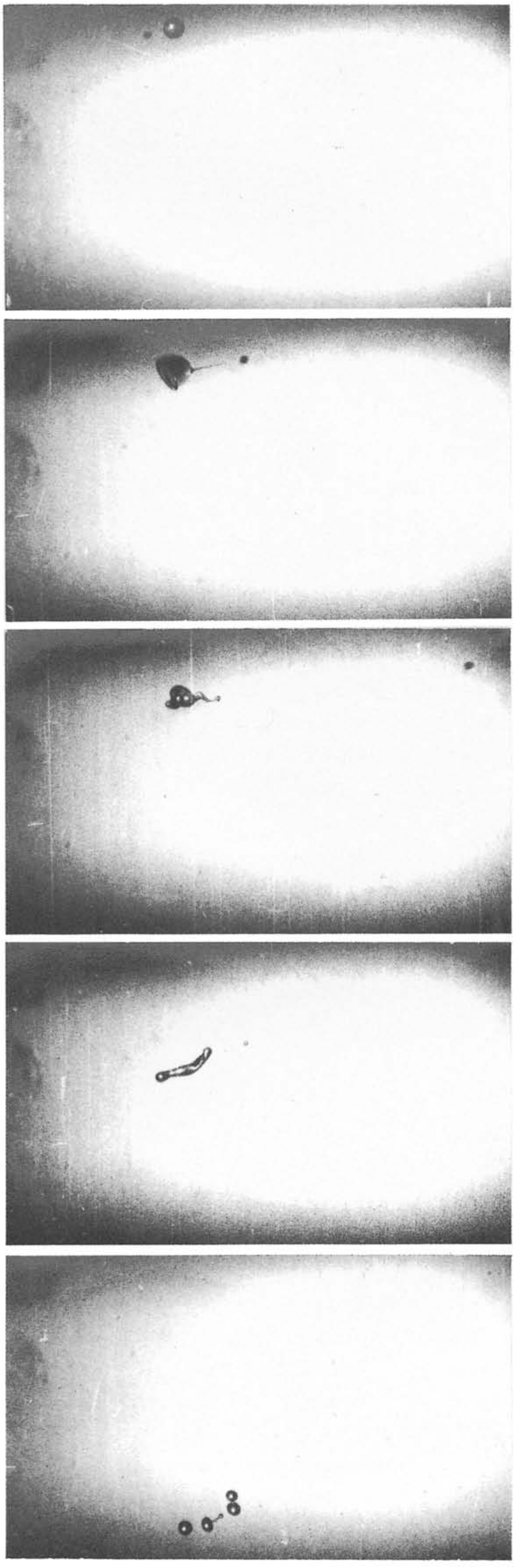

Figure 9. Interaction phases in the target destruction mode.

(4) Target destruction, i.e. it has decomposed into several large fragments, losing its individuality (figure 9).

In the case of the first three modes, relating to "mild" conditions of interaction, the weight method was used to determine the parameter Ψ_{ji}, since the fragments can be reliably separated from the targets being bombarded. At target destruction ("severe" mode) the weight method proved to be unacceptable, here the methods of filming and photography were used.

Capture was observed mainly at central impacts with small relative velocity, when projectiles of small and mean density collide with viscous drops. Destruction takes place within a sufficiently narrow range of interaction conditions (dense projectiles and drops of mean viscosities). The experimental data analysis has shown that the limits between the four modes studied can be determined most accurately on the coordinates $\mathrm{Re}^0_{ji} - \mathrm{We}^0_{ji}$ (figure 10), where $\mathrm{We}^0_{ji} = (\mathrm{Re}^0_{ji})^2/Lp_i \cdot \rho_s/\rho_L$, $\mathrm{Re}^0_{ji} = (U_j - u_i)\Delta_j \rho_L/\eta_L$.

In the case of the mild hydrodynamic modes, the coalescence and breakup parameter is conveniently presented as follows:

$$\Psi_{ji} = \Psi'_{ji} \frac{\rho_L}{\rho_s} + \Psi''_{ji}, \qquad [10]$$

where the first term allows for the variation of the liquid mass in the target, and the second for the solid particles capture by it (with $\Psi'_{ji} \leqslant 0$, $\Psi''_{ji} \geqslant 0$); the Ψ'_{ji} parameter is the relation of the target volume variation to the projectiles' volume colliding with it.

As shown in figure 11, the less dense projectiles cause the greatest target breakup (the opposite situation would be thought the more natural one). Evidently, the explanation is that the residence time of heavy particles in the target is smaller, so they cause less significant deformation of it. With increasing relative velocity, the target breakup intensifies. The probability of the capture of solid particles by the drops increases with the growth in the liquid viscosity and the relation between the sizes of the interacting particles. With an increase in the density of the projectiles and the relative velocity, the probability decreases.

For the interaction outcome, averaged by the midship section of the target, the following empirical dependences were obtained:

$$\Psi'_{ji} = 1 - 0.23(\mathrm{Re}^0_{ji})^{0.04}(\mathrm{We}^0_{ji})^{0.26}\left(\frac{\rho_s}{\rho_L}\right)^{-0.1}\left(\frac{\delta_i}{\Delta_j}\right)^{0.31}; \qquad [11]$$

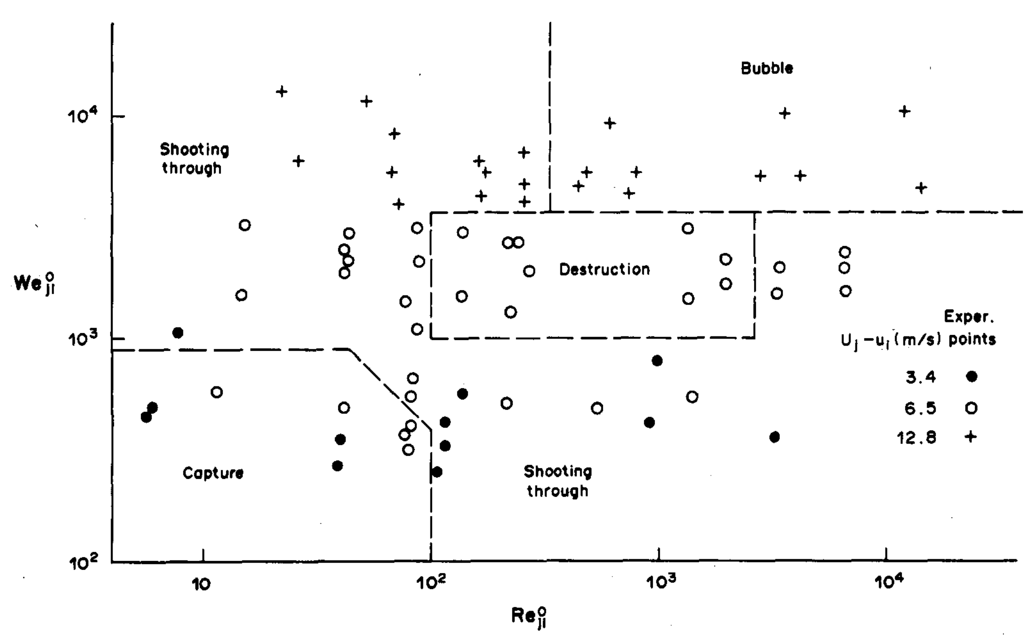

Figure 10. Diagram of the interaction modes.

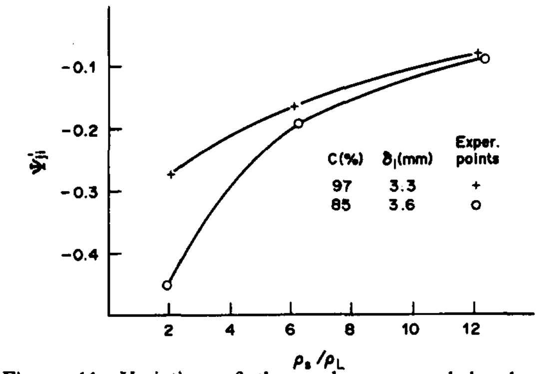

Figure 11. Variation of the coalescence and breakup parameter with the density relation of the particles.

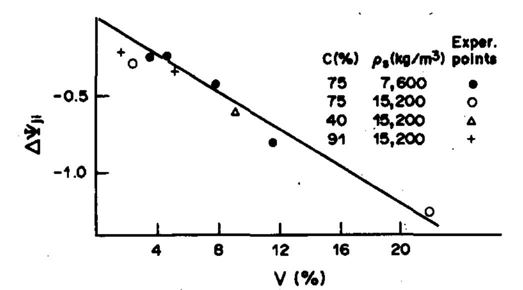

Figure 12. Effect of the solid inclusions concentration on the coalescence and breakup parameter.

and

$$\Psi''_{ji} = \begin{cases} 1 - 0.191 S_{ji}, & S_{ji} < 5.24; \\ 0, & S_{ji} \geqslant 5.24; \end{cases} \qquad [12]$$

$$S_{ji} = (\mathrm{Re}^0_{ji})^{0.19} (\mathrm{We}^0_{ji})^{0.17} \left(\frac{\rho_s}{\rho_L}\right)^{-0.12} \left(\frac{\delta_i}{\Delta_j}\right)^{-0.25};$$

in the range $6 \leqslant \mathrm{Re}^0_{ji} \leqslant 1.4 \cdot 10^4$, $240 \leqslant \mathrm{We}^0_{ji} \leqslant 13.3 \cdot 10^3$, $2.1 \leqslant \rho_s/\rho_L \leqslant 15.2$, $3 \leqslant \delta_i/\Delta_j \leqslant 5.6$.

In the severe modes, target destruction into several (from 2 to 6) fragments, approximately equal in size, was observed. The experiments showed that the larger and more viscous targets form fewer fragments, all other conditions being equal.

4.3. The initial parameters of fragments

The measurements showed that in the "shooting through" and destruction modes, the fragments' size distribution is approximated sufficiently well by the lognormal law [9]. Only the fragments formed behind the projectiles flying out of the target have been processed; the large fragments formed during the target breakup have not been allowed for. The following averaged distribution parameter values were obtained: $\ln \bar{\varepsilon} = -0.38$, $\ln \Sigma = 0.336$.

For the "shooting through" and destruction modes, the mean value of the liquid fragments' initial velocities was found to be $\bar{u}_k/U_j = 0.17$ at $32 \leqslant \mathrm{Re}^0_{ji} \leqslant 3400$, $1800 \leqslant \mathrm{We}^0_{ji} \leqslant 2800$.

Furthermore, the velocity U_k of the projectiles (it is more correct to call them the solid fragments) was measured during the escape from the drop targets in the same modes. The experimental data are described by the relation

$$\frac{\overline{U_k}}{U_j} = \frac{1 - 0.025\left(15 - \dfrac{\rho_s}{\rho_L}\right)}{\sqrt{1 - \left(\dfrac{2.75}{Lp_i}\right)}}. \qquad [13]$$

5. INTERACTION OF THE TWO-COMPONENT PARTICLES

Using the experimental apparatus in figure 5, experiments were performed to define the parameter $\tilde{\Psi}'_{ji}$ at collisions of solid projectiles with large particles of the first type—drops containing solid inclusions. To obtain two-component targets the apparatus was equipped with a tank from which fine sand, approximating monodisperse particles, was fed through a regulating feeder in water–glycerine solution in a cone funnel. The suspension was agitated by means of an activator. To improve the feeding of sand from the tank a vibrator was used. As before, the suspension breakup into monodisperse two-component particles was achieved by the superposition of pressure pulsations on the jet coming out of the capillary. The effect of the solid inclusions on the parameter Ψ_{ji} was evaluated by the discordance value $\Delta\Psi_{ji} = \tilde{\Psi}'_{ji} - \Psi'_{ji}$ (here Ψ'_{ji} was determined by [11], where the physical properties of the pure liquid were used in calculating the right-hand side). The diameter of the two-component monodisperse particles was varied within the range $\delta_i = 3.5$ to 5 mm. To prepare the suspension, quartz sand with particles of 160–315 μm size and $\rho_1 = 2774$ kg/m^3 density was used. The volume concentration of the solid inclusions in the drops was $V = 0$ to 0.22.

During the experiments it was noticed that the total volume of fragments formed during the interaction of projectiles with drops containing solid additions was greater than that during collisions with pure drops, all other conditions being equal. Figure 12 shows the dependence of $\Delta\Psi_{ji}$ on the concentration of solid inclusions in the drops. No evident separation of the experimental points into groups, by target viscosity or projectile density, in the range studied was found. The following correlation was obtained for $\Delta\Psi_{ji}$:

$$\Delta\Psi_{ji} = -6V \qquad [14]$$

at $26 \leqslant \mathrm{Re}^0_{ji} \leqslant 2000$, $1900 \leqslant \mathrm{We}^0_{ji} \leqslant 2600$, $6 \leqslant \rho_s/\rho_L \leqslant 14$, $3.7 \leqslant \delta_i/\Delta_j \leqslant 5$. The amount of solid particles in the fragments was estimated merely qualitatively (by sight). It increased with decreasing drop target viscosity. However, the amount of solid particles in the fragments was less than in the initial drops.

The experiments to determine the parameter $\tilde{\Phi}_{ji}$ during the interaction of the pure drops projectiles with the two-component particles targets were carried out with help of the experimental apparatus described by Podvysotsky & Shraiber (1984). The apparatus was re-equipped for working with a suspension. Both positive and negative values of $\Delta\Phi_{ji} = \tilde{\Phi}_{ji} - \Phi_{ji}$ were obtained ($|\Delta\Phi_{ji}| \leqslant 0.25$, the value Φ_{ji} was determined by [4] from the suspension physical properties). The averaged value of $\Delta\Phi_{ji}$ was close to zero over the whole experimental data array. Thus, the solid inclusions affect the difference in the coalescence and breakup parameter of drops with solid additions and that of drops of pure liquid only, so far as the change in the physical properties of the target substance in concerned.

Studies of the interaction of small particles of the second type with large free-falling pure drops were carried out on the experimental apparatus shown in figure 5. An ejection-type pneumatic sprayer was installed in the path of the solid particle between the projectile generator and the collision point. Particles approaching the target were covered with a liquid film deposited on their surfaces in the aerosol cloud. The experiments showed that a liquid mass content in the solid particle of 1% (we have not succeeded in raising this value on the experimental apparatus) affects neither the qualitative pattern of the interaction process nor the value of the parameter Ψ.

6. SOME NUMERICAL RESULTS

In accordance with the mathematical model presented in section 1 using the obtained experimental data (see [4]–[6] and [10]–[12]), computations of the three-phase polydisperse flow were carried out. We present here some results for a flow of mixture gas–magnesium drops–solid particles of magnesium oxide in a Laval nozzle (Shraiber & Klimov 1989). The nozzle contour consisted of an inlet part, outlined by an arc of a circle of radius $R_1 = 1.5r_*$, a conic subsonic part, with a half-angle of 30°, and a transonic part, an arc of radius $R_2 = 2r_*$ (r_* is the radius of the minimum section). The fractional composition of the initial particles is given in table 2 (h_i, H_i are the mass parts of the fractions). According to figure 13 (therein and in figures 14 and 15, x values are referenced to r_*), it is evident that the three-phase polydisperse flow is accompanied by intensive particle interaction. In the subsonic part the mass of the drops is increased 2–3 times, since the velocities of the interfractional slip are not great in this part and the Φ_{ji} and Ψ_{ji} values are near to unity (see [2], [4], [11] and [12]). In the transonic part the slip is considerably greater, and the breakup of large drops is observed. It is interesting to note that in the outlet section the m_{10} value

Table 2. Composition of the initial condensate

	i									
	1	2	3	4	5	6	7	8	9	10
$\delta_i \cdot 10^6$ (m)	5	20	40	55	70	90	105	120	135	150
$h_i \cdot 10^3$	6	15	23	91	120	200	355	158	24	8
$\Delta_i \cdot 10^6$ (m)	2	10	100							
$H_i \cdot 10^2$	23	71	6							

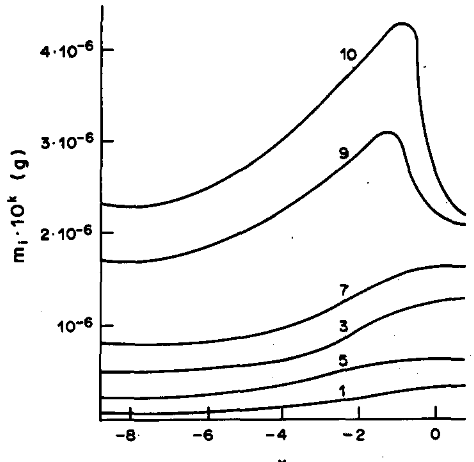

Figure 13. Variation of the mass of the drop along the flow length (here and in figures 14 and 15 the curve numbers correspond to table 2): $K = 3$ for curve 1; $K = 1$ for curve 3; $K = 0$ for other curves.

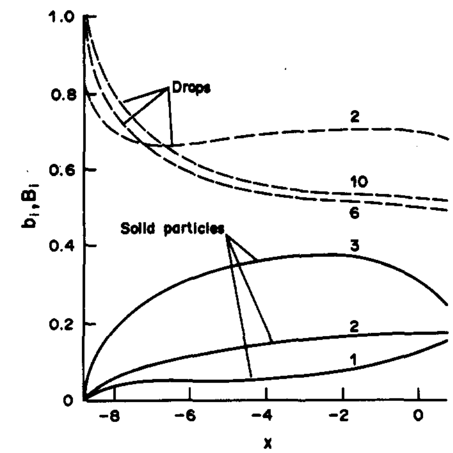

Figure 14. Liquid mass content in the drops and in the solid particles.

is less than the inlet value, and the mass of the drops in the three largest fractions become almost equal. The flow, to a certain extent, is self-similar relative to the initial drop sizes, as the large drops are subjected to more intensive breakup.

Figure 14 illustrates the change in the component composition of particles of some fractions along the flow length. It is clear that interaction is accompanied by a noticeable mass transfer between particles of a different nature: b_i values are decreased by up to 0.55–0.7; and B_i values are increased by up to 0.1–0.4. It is interesting that in the transonic part the B_3 value is decreasing—here breakup of the liquid shell of the M_3 particles prevails. In figure 15, a phenomenon unusual

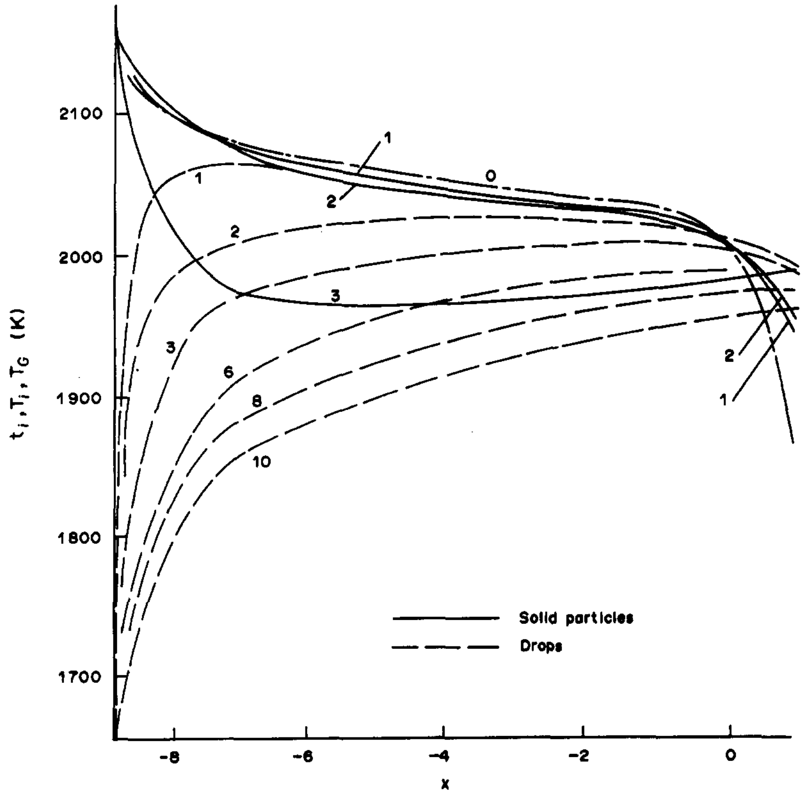

Figure 15. Variation of the temperature of the gas (0) and particles along the flow length.

in multiphase flows draws our attention: solid lines 1 and 2 intersect twice with the curve of the gas. This is due to the formation of a considerable amount of these fractions at "cold" large drops breakup.

7. CONCLUSIONS

The main results of the present work are as follows:

(a) The interaction of fast-moving small drops with large solid particles is always accompanied by liquid breakup and the formation of a certain number of fragments. The material balance of the interaction is expresssed by [6]–[8].
(b) The existence of four modes of interaction of the small solid particles with the large drops was determined: (1) projectile capture by the target; (2) "shooting through"; (3) gas bubble formation; (4) target destruction. For modes (1)–(3) the target mass change is described by [10]–[12].
(c) Ψ-interaction in the presence of solid inclusions in the drop target results in a noticeable intensification of its breakup, in accordance with [14]. No effect of this factor on the material balance of the Φ-interaction has been found.
(d) The fractional composition of fragments is well-approximated by a lognormal distribution. The initial velocity of the fragments is several times less than the projectile velocity.
(e) The interaction of particles considerably affects the changes in the basic parameters of three-phase polydisperse flow.

The results described in this paper can be used in analysing the transfer processes in different systems with three-phase polydisperse flows, where conditions similar to those in our experiments are realized. At the same time, the data obtained apparently do not apply to the modelling of the interaction of particles in the atmosphere.

Acknowledgements—The authors are grateful to V. L. Klimov for useful discussions on this work and to N. S. Slatvinskaya for her help in carrying it out.

REFERENCES

BABUKHA, G. L. & SHRAIBER, A. A. 1972 *Polydisperse Material Particles Interaction in Two-phase Flows*. Naukova Dumka Press, Kiev (in Russian).

BRAZIER-SMITH, P. R., JENNINGS, S. G. & LATHAM, J. 1972 The interaction of falling water drops: coalescence. *Proc. R. Soc. Lond.* **A326**, 393–408.

CZYS, R. R. & OCHS, H. T. 1988 The influence of charge on the coalescence of water drops. *J. Atmos. Sci.* **45**, 3161–3168.

DAVIS, A. M. J. & BRENNER, H. 1981 Emulsions containing a third solid internal phase. *Proc. Am. Soc. Civ. Engrs, J. Engng Mech. Div.* **107**, 609–621.

GAWRONSKI, R. & ROSZAK, J. 1979 Drop sizes in liquid–liquid co-current flow through fluidized beds. *Inz. Chem.* **9**, 88–98.

GILLESPIE, D. T. 1975 Three models for coalescence growth of cloud drops. *J. Atmos. Sci.* **32**, 600–607.

KHORGUANY, V. G. 1984 *Microphysics of Formation and Growth of Hail*. Gidrometeoizdat, St Petersburg (in Russian).

LEW, J. K., MONTAGUE, D. C., PRUPPACHER, H. R. & RASMUSSEN, R. M. 1986 A wind tunnel investigation on the riming of snow flakes. Part I: Porous disks and large stellars. *J. Atmos. Sci.* **43**, 2392–2409.

MARTIN, J. J., WANG, P. K. & PRUPPACHER, H. R. 1980 A theoretical study of the effect of electric charges on the efficiency with which aerosol particles are collected by ice crystal plates. *J. Colloid Interface Sci.* **78**, 44–56.

NIGMATULIN, R. I. 1987 *Dynamics of Multiphase Media*. Nauka Press, Moscow (in Russian).

OCHS, H. T., CZYS, R. R. & BEARD, K. V. 1986 Laboratory measurements of collection efficiencies for accretion. *J. Atmos. Sci.* **41**, 863–867.

PETELA, R. & ZAJDEL, A. 1980 Calculation of a mean droplet diameter of an atomized mixture of dust and liquid. *Fuel* **59,** 795–798.

PILCH, M. & ERDMAN, C. A. 1987 Use of breakup time data and velocity history data to predict the maximum size of stable fragments for acceleration-induced breakup of a liquid drop. *Int. J. Multiphase Flow* **13,** 741–757.

PODVYSOTSKY, A. M. & SHRAIBER, A. A. 1984 Coalescence and breakup of drops in two-phase flows. *Int. J. Multiphase Flow* **10,** 195–209.

PODVYSOTSKY, A. M., DUBROVSKY, V. V. & SLATVINSKAYA, N. S. 1990 Experimental study of the peculiarities of mass transfer at interaction of drops with solid particles. In *Teplo- i energosberezheniye, Teplometriya*, pp. 17–24. Inst. of Energy Saving Problems, Ukz. Acad. Sci., Kiev (in Russian).

PRUPPACHER, H. R. & KLETT, J. D. 1978 *Microphysics of Clouds and Precipitation.* Reidel, Dordrecht.

RASMUSSEN, R. M. & HEYMSFIELD, A. J. 1987 Melting and shedding of graupel and hail. Part I: model physics. *J. Atmos. Sci.* **44,** 2754–2763.

SAUTER, D. P. & WANG, P. K. 1989 An experimental study of the scavenging of aerosol particles by natural snow crystals. *J. Atmos. Sci.* **46,** 1650–1655.

SHRAIBER, A. A. 1988 Multiphase polydisperse flows with variable fractional composition of discrete inclusions. In *Itogi Nauki i Tekhniki. Komplexnyye i Spetsialnyye Razdely Mehaniki*, Vol. 3, pp. 3–80. VINITI Press, Moscow (in Russian).

SHRAIBER, A. A. & DUBROVSKY, V. V. 1986 Numerical study of three-phase polydisperse flow features with variable composition of discrete inclusions. In *Teplo- i Massoobmennyye Protsessy*, pp. 60–68. Naukova Dumka Press, Kiev (in Russian).

SHRAIBER, A. A. & KLIMOV, V. L. 1989 Three-phase flow with coalescence, breakup, vaporization and burning of particles. In *Heat/Mass Transfer—MIF*, Sect. 3, pp. 185–196. A. V. Luikov Inst. of Heat & Mass Transfer, Byelorussian Acad. Sci., Minsk (in Russian).

SMIRNOV, V. I. 1987 Microstructure of clouds and precipitation. In *Itogi Nauki i Tekhniki. Meteorologia i Klimatologia*, Vol. 15, pp. 3–193. VINITI Press, Moscow (in Russian).

STERNIN, L. YE., MASLOW, B. N., SHRAIBER, A. A. & PODVYSOTSKY, A. M. 1980 *Two-phase Mono- and Polydisperse Flows of Gas with Particles.* Mashinostroyeniye Press, Moscow (in Russian).

STULOV, L. D., MURASHKEVICH, F. I. & FUCHS, N. 1978 The efficiency of collision of solid aerosol particles with water surfaces. *J. Aerosol Sci.* **9,** 1–6.

VASENIN, I. M., ARKHIPOV, V. A., BUTOV, V. G., GLAZUNOV, A. A. & TROFIMOV, V. F. 1986 *Gas Dynamics of Two-phase Flows in Nozzles.* Tomsk University Press, Tomsk (in Russian).

ZAVADSKY, V. A. 1982 Study of motion of a single solid particle with variable mass in a flame of sprayed liquid. In *Teplo- i Massoperenos v Dispersnyh Sistemah*, pp. 136–149. A. V. Luikov Inst. of Heat & Mass Transfer, Byelorussian Acad. Sci., Minsk (in Russian).